JOURNAL OF CATALYSIS 142, 664–671 (1993)

Formation of Coke in the Disproportionation of *n*-Propylbenzene on Zeolites

SHANG-BIN LIU,*[,1] S. PRASAD,* JIN-FU WU,* LONG-JA MA,* TRAN-CHIN YANG,* JAW-TANG CHIOU,† JEN-YAW CHANG,† AND TSENG-CHANG TSAI†

*Institute of Atomic and Molecular Sciences, Academia Sinica, P. O. Box 23-166, Taipei, Taiwan 10764, Republic of China; and †Refining and Manufacturing Research Center, Chinese Petroleum Corporation, Chia-Yi, Taiwan 60036, Republic of China

Received November 16, 1992; revised March 22, 1993

We investigated the formation of coke on zeolitic catalysts in the disproportionation of *n*-propylbenzene by means of ^{129}Xe, ^{27}Al, and ^{13}C NMR spectroscopy. According to ^{13}C CP-MAS (proton cross polarization with magic angle spinning) spectra, the coke formed in USY and ZSM-5 zeolites was classified into aliphatics and aromatics. It was found that aliphatic coke could be removed by a simple evacuation procedure. The location of the coke determined from ^{129}Xe NMR spectra and xenon adsorption isotherms varied with the zeolite catalysts. For zeolite USY, the coke was formed inside the supercages and is mainly polyaromatic. For zeolite ZSM-5, the coke is alkykaromatic and tended to deposit at the openings of the channels rather than at their intersections. In regard to the mechanism, the reaction on USY followed bimolecular kinetics, whereas on ZSM-5 the reaction was monomolecular.

INTRODUCTION

The formation and nature of carbonaceous residues (coke) in catalytic reactions affect the rate of deactivation of the acidic zeolite catalysts. Highly siliceous zeolites such as ultra-stable Y (USY) and ZSM-5, although having an unique advantage in catalytic-cracking processes, are vulnerable to coke due to poisoning of catalyst sites and blocking of pores. Although the activity of the zeolites can be regenerated by combustion of coke at an elevated temperature, the process is normally controlled by the characteristics of the coke and commonly resulted in hydrothermal deactivation and collapse of the zeolitic framework structure. Hence a detailed understanding and control of coke formation are of great concern for both industrial applications and academic research.

Coking on and deactivation of zeolites have been comprehensively reviewed (*1–3*). The rate of deposition of coke and its selectivity have been known to depend not only on the operating conditions (e.g., reaction time, temperature, pressure, nature of the reactant, etc.) but also on the zeolitic pore structure (*4, 5*). The pore structure of zeolites affect the rate of coking and its deactivation effect. The effect of deactivation of coke is more pronounced on zeolites having large cavities with small apertures than on those having interconnecting channels without cavities (*1, 2, 6*). As a result, steric constraints exerted by the pore openings of ZSM-5 on formation of coke are more pronounced than on the supercages of zeolite Y, hence resulting in less deactivation of ZSM-5. Although the acidity of the zeolites also plays a significant role on the rate of coking, it is sometimes difficult to discriminate between this effect and that of the pore structure. In terms of reaction mechanism, the transition state shape selectivity has been disclosed (*7*), however, that of disproportionation reactions was not resolved un-

[1] To whom correspondence should be addressed.

0021-9517/93 $5.00

til recently (*8, 9*). It was found (*9*) that zeolite USY catalyzes a bimolecular reaction in n-propylbenzene disproportionation whereas ZSM-5 favors a monomolecular mechanism. Furthermore, the bimolecular reaction is suppressed on zeolites having ten-membered rings (*9–12*). Various mechanisms hence result in various reaction intermediates and/or coke precursors.

Although the formation of coke from hydrocarbon reactions on acidic catalysts has been reported, the origin and nature of coke have been studied less extensively. Among the many spectral techniques applied to coked zeolitic catalysts, ^{129}Xe (*13–17*) and ^{13}C (*17–23*) NMR spectroscopy have proved useful. Our objective was to investigate the effects of zeolitic pore structure on the reaction mechanism, location, and nature of coke formed in the disproportionation reaction. We used ^{13}C CP-MAS NMR, ^{27}Al MAS NMR, and measurement of isotherms and ^{129}Xe NMR of adsorbed xenon in conjunction with thermogravimetry.

EXPERIMENTAL

Zeolite H–ZSM-5 was prepared according to the procedure of Chao *et al.* (*24*). Zeolite H–USY was supplied by Tosho Company. The samples of coked zeolite from disproportionation of *n*-propylbenzene were obtained with time-on-steam of 3 h; detailed procedures resemble those reported previously (*9*).

Thermogravimetric analysis (TGA) was conducted on a Dupont 951 thermogravimeter with the conditions: sample weight, 30 mg; reference sample, alumina; flowing gas, atmospheric N_2; heating rate, 10°C min^{-1}; ultimate temperature, 950°C.

NMR measurements were performed on a Bruker MSL-300 spectrometer. The ^{13}C CP-MAS NMR spectra were obtained with proton decoupling at a frequency of 75.47 MHz. Typically 40,000 free-induction decay (FID) signals were accumulated every 0.6 s at room temperature (22°C). The ^{13}C chemical shifts were measured relative to tetramethylsilane (TMS). The ^{27}Al MAS NMR spectra were recorded at 78.21 MHz using a single-pulse scheme with a recycle delay of 0.3 s. The ^{27}Al chemical shifts were referred to saturated $AlCl_3$ solution. For the MAS experiments, samples were enclosed in a 7-mm rotor and a spinning frequency ca. 5 kHz was used. The ^{129}Xe NMR spectra were obtained at 83.01 MHz; normally 1000–20,000 FID signals were accumulated at 0.3-s intervals. ^{129}Xe NMR spectra and xenon adsorption isotherms were obtained at room temperature; the ^{129}Xe NMR experiments are described elsewhere (*25*).

TABLE 1

Reaction Conditions and Coke Content in Disproportionation of *n*-Propylbenzene on USY and ZSM-5 Zeolites

Zeolite	USY(1)	USY(2)	ZSM-5(1)
Crystalline size (μm)	1.5	1.5	0.1
SiO_2/Al_2O_3 ratio	14.5	14.5	35.8
Reaction conditions			
Temperature (°C)	200	280	200
WHSV (g/h · g · cat.)	4.9	3.6	9.4
Conversion (wt%)	5.0	20.0	5.0
Coke contents (wt%)			
Coke I	4.5	3.9	3.0
Coke II	0.1	0.2	0.2
Total coke	4.6	4.1	3.2

RESULTS AND DISCUSSION

The properties of coked samples prepared under various conditions are given in Table 1. Coking is expected to be influenced by the reaction temperature as well as the crystalline size of zeolites. In the context of this study, however, qualitative comparisons of the coke deposition between USY(1) and USY(2) and that of USY(1) and ZSM-5(1) can be made based on the conclusions drawn by Tsai and Wang (*9*) from the identical systems. For the coke formation in *n*-propylbenzene disproportionation, Tsai and Wang (*9*) found that the respective reaction mechanism remains unchanged in the range of reaction temperature between 200 and 275°C for USY and ZSM-5. For ZSM-5, the

same authors further revealed that while the size of crystalline has a substantial influence on product isomer selectivity, it plays a minor role in determining the mechanism of disproportionation reaction.

In Table 1, the amount of total coke deposited on USY decreases from 4.6 to 4.1 wt% upon increasing conversion levels from 5 to 20 wt%. This observation is at variance with disproportionation of toluene on USY under different reaction conditions (*26*). By comparison, ZSM-5(1) has less total coke deposited than USY at the same conversion level of 5 wt%, in accordance with the notion that the rate of coking depends on the porous structure of the zeolites. In this context, cokes have been classified into two types based on their temperature of deposition. Coke I, "volatile coke," refers to those that may be removed at temperature $T <$ 450°C. Coke II, "hard coke," refers to the coke desorbed at 450°C $\leq T \leq$ 950°C. Coke II is desorbed at greater temperatures because the bulky coke molecules is less volatile. For USY, the amount of coke II increased evidently with increasing severity of reaction. In contrast, under the same conditions, the increased content of coke II on ZSM-5 vs USY reveals the selective porous structure of the zeolites.

^{13}C NMR spectra of coked USY and ZSM-5 both (Fig. 1) exhibit two distinct groups of resonance lines that are assigned (*26, 27*) to aliphatics (0-50 ppm) and aromatics (110–150 ppm). The lines of aliphatic species correspond to terminal methyl (13 ppm), penultimate methylene (25 ppm), and other methylene groups (38–50 ppm). Comparison of the spectra in Figs. 1a and 1b indicates that the relative intensity of lines due to aliphatic species decreases notably with increasing reaction temperature (hereafter denoted T_r) as less condensable coke (coke I) occurred at greater T_r. Neuber *et al.* (*20*) reported similarly for reaction of methylnaphthalene on zeolite Beta. Upon dehydration (dehydration temperature T_d = 180°C, 20 h) of USY(1) under vacuum, the overall features and relative intensities of

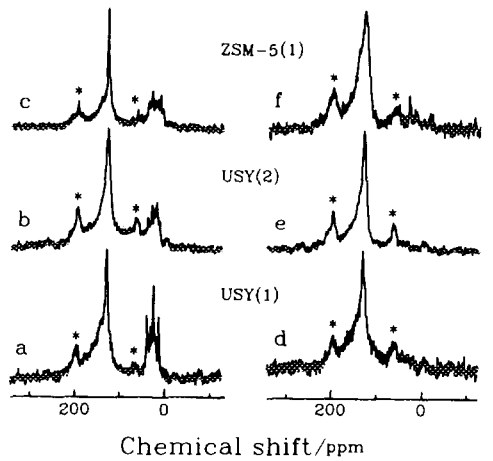

FIG. 1. The ^{13}C CP-MAS NMR spectra of coked USY and ZSM-5. Sample spinning frequency 5 kHz; the spinning sidebands are indicated by asterisks: (a) and (b) without dehydration treatment, (c) T_d = 180°C, 30 h; (d)–(f) T_d = 450 °C, 20 h.

the ^{13}C NMR spectra (not shown) remain almost unchanged relative to Fig. 1a except for a slight broadening of the aromatics line. This broadening of the aromatics line upon dehydration with $T_d < T_r$ is a priori related to the rearrangement of coke precursors. Further increasing the temperature of dehydration to 450°C, the aliphatic resonances vanish completely (Figs. 1d and 1e). This simple vacuum treatment to remove aliphatic coke precursors deviates from customary procedures in which mixtures of ozone and air are used (*21, 28*). The remaining broad peak centered at 128 ppm is assigned to polyaromatic coke precursors.

The ^{13}C NMR spectrum of coked ZSM-5(1) obtained after dehydration at T_d = 180°C (30 h) under vacuum appears in Fig. 1c; two distinct groups of resonances similar to those of coked USY are observed. However, the lines due to aromatic species on ZSM-5(1) in Fig. 1c appears narrower than those for USY(1) before dehydration (Fig. 1a). We attribute the former to lighter aromatic compounds and the latter to more condensed aromatic rings (*2, 29*). Upon dehydration of ZSM-5(1) at 450°C under vacuum

(Fig. 1f), only one line at 30 ppm remained and the aromatic peak at 128 ppm broadened. The line at 30 ppm is ascribed to methyl groups in substituted polyaromatic compounds (*30, 31*), whereas the broad line at 128 ppm may be due to the self-condensation of coke precursors (likely methyl-substituted aromatics).

These ^{13}C NMR results support the hypothesis that the mechanism of disproportionation depends on the types of zeolites, as Tsai and Wang proposed (*9*), that is, ZSM-5 catalyzes monomolecular disproportionation, whereas USY catalyzes bimolecular disproportionation mechanism. They stated also that the reaction intermediates for ZSM-5 are propyl ions and benzene molecules but ethylphenylcarbonium ions and biphenylalkyl ions for USY. Coke being the derivative of reaction intermediates, the propyl ions possibly cyclise within the pores of ZSM-5 to form methyl substituted polyaromatics that deposit as coke. Accordingly, the coke deposited on ZSM-5(1) has greater molecular symmetry that resulted in a narrower aromatic line (Fig. 1c), in contrast with the broader line for USY (Fig. 1a) from which various coke compounds via phenyl ions were formed.

Figure 2 shows ^{129}Xe NMR spectra of xenon (loading pressure 300 Torr) adsorbed in the supercage of dehydrated (T_d = 450°C) parent and coked USY. The observed ^{129}Xe resonance line in Fig. 2a, chemical shift δ = 68 ppm, arises from the collision of xenon atoms with the zeolite walls and from xenon–xenon interactions within the parent USY supercage. The narrow line in Fig. 2a indicates that the ^{129}Xe resonance detects an average environment on the time scale of the NMR measurements (*25*). In Figs. 2b and 2c, the migration of xenon is hindered by coke deposited within the USY supercage and hence the broadening of the ^{129}Xe line. The increase in ^{129}Xe chemical shift in the coked samples vs uncoked parent USY is due to the presence of coke within the USY supercage, hence a decrease in zeolitic void space and an additional contribution from xenon–coke interactions (*14*). For coked USY(1), a broader line appeared at δ = 75 ppm which overlapped the narrower peak (δ = 68 ppm) of the parent USY that we assign to arise from coke-containing supercages. The spectrum indicates that coke is heterogeneously deposited on USY(1). As the reaction temperature becomes greater, shown in Fig. 2c for USY(2), a broad and symmetric peak located at δ = 79 ppm therefore indicates homogeneous coke deposit (*14*) within the supercages. The greater chemical shift observed in USY(2) relative to USY(1) also signifies that USY(2) contains more coke II than USY(1), in agreement with the TGA results. Similar results were obtained for coked USY samples for T_d = 250°C. ^{129}Xe NMR spectra of xenon (pressure 300 Torr) adsorbed in the voids of ZSM-5(1) appear in Figs. 2d–2f for various T_d. The broadening of the ^{129}Xe line with increasing T_d is a priori related to the rearrangement of coke precursors.

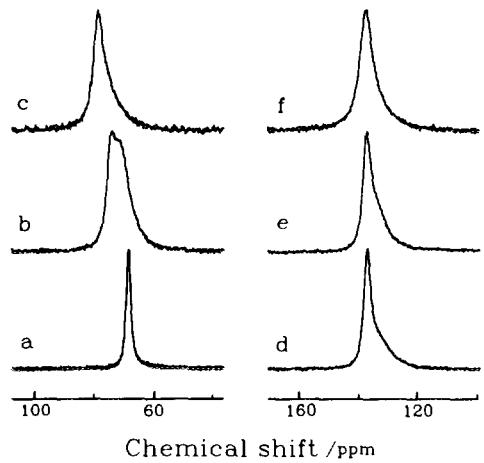

FIG. 2. Comparison of ^{129}Xe NMR spectra (xenon pressure 300 Torr) for various USY samples under the same T_d = 450°C and for ZSM-5(1) sample under various T_d: (a) parent USY, (b) USY(1), (c) USY(2); (d)–(f) ZSM-5(1), T_d = 180, 250, and 450°C, respectively.

The xenon adsorption isotherms for samples prepared and treated under various conditions appear in Fig. 3. In Fig. 3a, the isotherms of USY(1) and USY(2) both in-

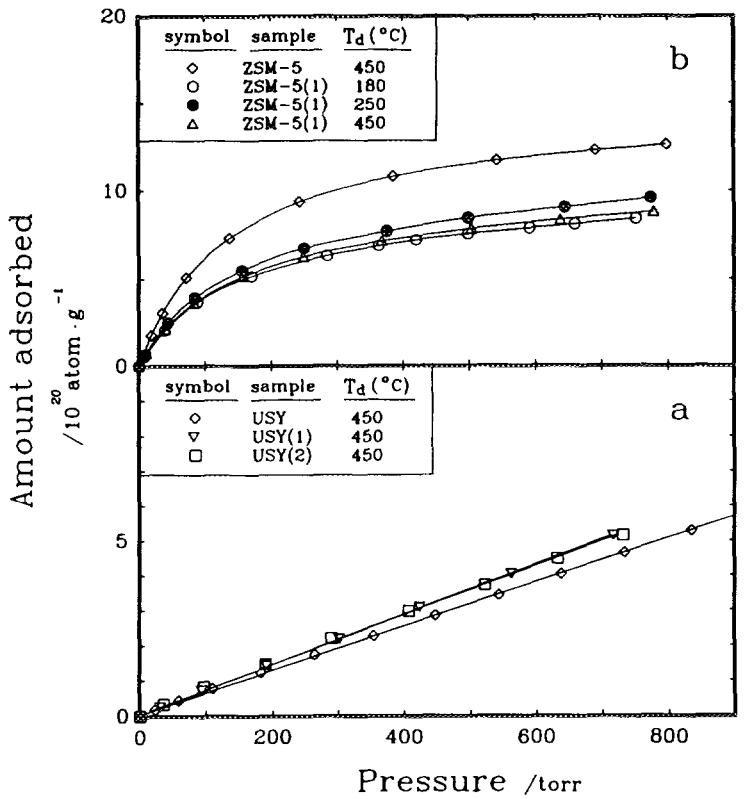

FIG. 3. Room-temperature xenon adsorption isotherms of parent (fresh) and coked zeolites under various T_d: (a) USY and (b) ZSM-5.

crease linearly with xenon pressure similar to that of parent USY. The fact that the slopes of the adsorption curves of USY(1) and USY(2) are the same indicates that the respective adsorption strength for the coked samples are the same even though the distribution and amount of coke in these samples differ (*vide supra*, ^{13}C and ^{129}Xe NMR and TGA results). The slight increase of slope in coked USY relative to parent USY might be due to increased overall adsorption strength in the presence of coke (*13, 17*). This behavior is in contrast to that of ZSM-5(1) in Fig. 3b in which the Langmuir-type isotherms of the coked samples at various T_d all show a marked decrease relative to that of parent ZSM-5. A slightly increased adsorption of T_d = 250°C relative to T_d = 180°C sample arose from the desorption of coke I, whereas the decreased adsorption upon temperature of dehydration increased from 250 to 450°C may be attributed to the condensation of coke precursors to form methyl-substituted aromatic compounds. These results therefore indicate a rearrangement of coke precursors within zeolitic pores, consistent with the ^{13}C NMR results.

In Fig. 4, ^{129}Xe chemical shifts measured at various pressures of xenon are plotted against xenon loading in conjunction with the xenon isotherm data. The ^{129}Xe chemical shift is described as the sum of three terms (*14, 32, 33*),

$$\delta = \delta_0 + \delta_e + \delta_s + \sigma_{xe-xe} \cdot \rho_{xe},$$

in which $\delta_0 = 0$ is the reference, and δ_e, the shift that arises from the electric field of the

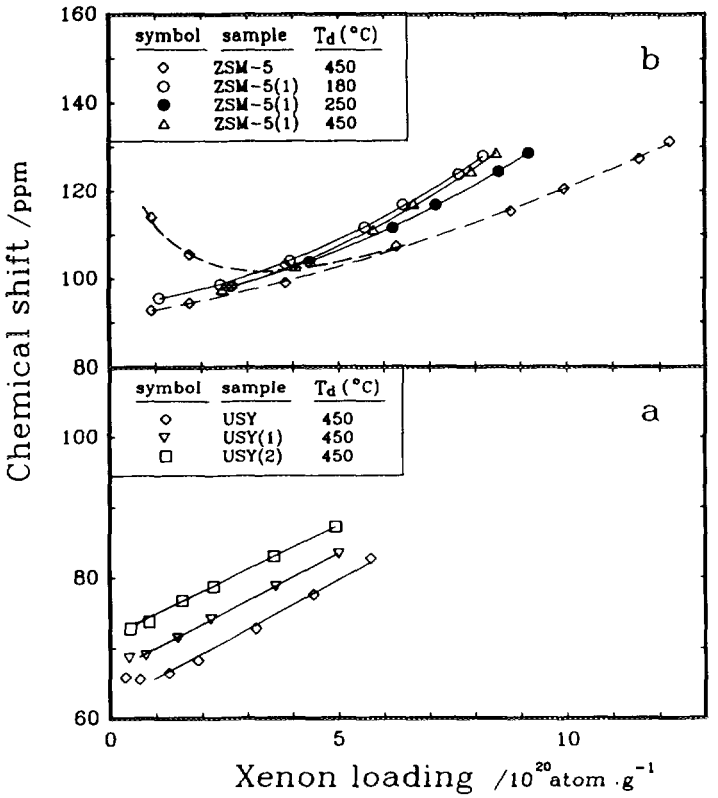

FIG. 4. Variation of ^{129}Xe NMR chemical shift with the xenon loading for parent and coked zeolites under various T_d: (a) USY and (b) ZSM-5.

monovalent cation, can be neglected (*33*) or at least have the same contribution for each zeolite sample. As far as qualitative interpretation of ^{129}Xe chemical shift for individual zeolite is concerned, the δ_e term plays a minor role in this context. δ_s, the shift at zero xenon loading, represents in turn the sum of two contributions, $\delta_s = \delta_{sz} + \delta_{sc}$. The term δ_{sz} arises from the interactions between xenon and the zeolite walls in the absence of coke. The term δ_{sc} arises from the interactions between xenon and coke deposited within the zeolitic pores. The last term, characteristic of xenon–xenon interactions in which binary collisions of xenon atoms dominate, is proportional to the density of adsorbed xenon (ρ_{xe}); the slope of the plot δ vs ρ_{xe} at a sufficiently great density of xenon therefore yields σ_{xe-xe} which depends on the xenon–xenon interactions.

In Fig. 4a, that the slopes σ_{xe-xe} of the parent and coked USY samples are nearly equal indicates that the xenon–xenon interaction within the zeolitic pores is invariant of deposited coke. In contrast, that the value of δ_s increases with increasing T_r indicates decreased zeolitic void space and increased xenon–coke interactions due to coke II in increased amount, as expected. In Fig. 4b, a nonlinear increase of ^{129}Xe chemical shift with xenon loading is evident for ZSM-5(1) samples treated at varous T_d and for parent ZSM-5. At small xenon loadings ($< 6 \times 10^{20}$ atom g^{-1}), when the xenon–zeolite interaction (δ_{sz}) dominated the contributions of δ, two overlapping lines were observed for parent ZSM-5 representing the two environments (Figs. 5a–5c). At greater loadings of xenon, when xenon–xenon interactions become more important rapid chemical ex-

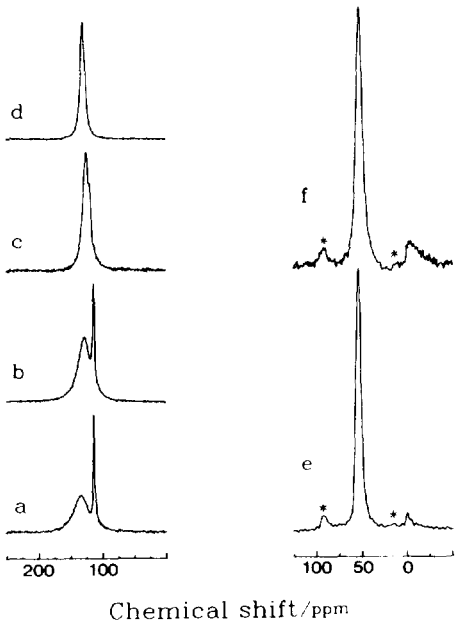

FIG. 5. Left: ^{129}Xe NMR spectra of parent ZSM-5 with various xenon loadings (a) 10, (b) 20, (c) 50, and (d) 100 Torr. Right: ^{27}Al MAS NMR spectra of (e) parent ZSM-5 and (f) ZSM-5(1), sample spinning frequency 5 kHz (spinning sidebands denoted by asterisks). The peak located at ca. 56 ppm arises from tetrahedral Al, whereas the peak located near 0 ppm arises from octahedral Al.

change resulted in a single line, as shown in Fig. 5d for xenon loading pressure of 100 Torr. It is puzzling that, while the split of ^{129}Xe NMR line at small xenon loading is commonly observed for H–ZSM-5 with various SiO_2/Al_2O_3 ratio in this laboratory (to be published), such an observation was absent for Na–ZSM-5 except for SiO_2/Al_2O_3 = 33.5 (*34*). For the coked ZSM-5(1) sample with different T_d, only one line was observed and the chemical shift curves all merged to the lower curve of parent ZSM-5. Similar behavior has been observed by Bonardet *et al.* (*35*) for conversion of methanol and acetone on H–ZSM-5; these authors attributed the upper curve in parent ZSM-5 to the presence of octahedral (or extraframework) aluminum which remained in the channel and acted as adsorption sites. However, our ^{27}Al MAS NMR spectra in Figs. 5e and 5f showed a slightly more intense octahedral Al line (near 0 ppm) for coked ZSM-5(1) relative to parent ZSM-5. Our results therefore contradict to the conclusion of Bonardet *et al.*

The site at which coke formation takes place in ZSM-5 is unresolved (*1–3*). For benzene adsorbed on ZSM-5 (*36*) and silicalite (*37*), two coking sites have been proposed, namely at the midchannel position and at the channel intersection. Hashimoto *et al.* (*38*) observed in ZSM-5 zeolite that coke is deposited mainly on the outer surface of the crystallite for methanol-to-gasoline, whereas for the alkylation of toluene with methanol coke is deposited mainly within the crystallite. Our xenon adsorption data and ^{129}Xe NMR results indicate that, at small concentrations of coke, the coke tends to deposit within the crystallite. According to the ^{129}Xe NMR chemical shift data for parent ZSM-5, we attribute the two chemical shift curves at low xenon loading to xenon adsorbed at two chemically non-equivalent sites. Accordingly, the upper curve corresponding to the larger chemical shift and hence smaller mean-free-path for xenon arises from xenon in the openings of the pores or midchannel positions, whereas the lower curve arises from xenon in the channel intersections which possess larger void space for xenon hence resulting in a smaller chemical shift. For the coked ZSM-5(1) sample with varied T_d, the fact that the chemical shift curves all merge to the lower curve of parent ZSM-5 at small xenon loadings indicates that coke tends to deposit at the midchannel positions instead of channel intersections. Moreover, at greater xenon loadings, the slope of the chemical shift curve for a sample treated at T_d = 180°C was slightly decreased relative to 250°C, and increased at T_d = 450°C, in accord with the notion that aliphatic residues are removed whereas polyaromatic compounds are formed upon consecutive dehydration. This observation agrees with earlier results.

CONCLUSIONS

The formation and composition of coke in disproportionation reaction depends not

only on the reaction conditions but also on the type of zeolite. The disproportionation of *n*-propylbenzene follows a bimolecular mechanism on zeolite USY, which retained polyaromatic coke, but a monomolecular mechanism on ZSM-5, for which the retained coke is alkylaromatic in nature.

The ^{13}C and ^{129}Xe NMR results revealed that the distribution of coke deposited on USY depends on the reaction temperature; the coke is located mostly in the zeolitic pores. For coked ZSM-5, a rearrangement of coke upon dehydration is observed; the coke tends to deposit at the midchannel positions instead of channel intersections.

ACKNOWLEDGMENTS

The authors express their appreciation to Professor Ikai Wang for stimulating discussions. The support of this work by the National Science Council (Grant NSC82-0208-M001-047) and the Chinese Petroleum Corporation of the Republic of China are gratefully acknowledged.

REFERENCES

1. Bhatia, S., Beltramini, J., and Do, D. D., *Catal. Rev.-Sci. Eng.* **31,** 431 (1989-90).
2. Guisnet, M., and Magnoux, P., *Appl. Catal.* **54,** 1 (1989).
3. Karge, H. G., *Stud. Surf. Sci. Catal.* **58,** 531 (1991).
4. Rollman, L. D., and Walsh, D. E., *J. Catal.* **56,** 139 (1979).
5. Olson, D. H., and Haag, W. O., *ACS Symp. Ser.* **248,** 275 (1984).
6. Derouane, E. G., and Gabelica, Z., *J. Catal.* **65,** 486 (1980).
7. Csicsery, S. M., *Zeolites* **4,** 202 (1984), and references therein.
8. Amelse, J. A., *Stud. Surf. Sci. Catal.* **38,** 165 (1988).
9. Tsai, T. C., and Wang, I., *J. Catal.* **133,** 136 (1992).
10. Martens, J. A., Perez-Pariente, J., Sastre, E., Corma, A., and Jacobs, P. A., *Appl. Catal.* **45,** 85 (1988).
11. Kumar, R., Rao, G. N., and Ratnasamy, P., *Stud. Surf. Sci. Catal.* **49,** 1141 (1989).
12. Tsai, T. C., Ay, C. L., and Wang, I., *Appl. Catal.* **77,** 199 (1991).
13. Ito, T., Bonardt, J. L., Fraissard, J., Nagy, J. B., Andre, C., Gabelica, Z., and Derouane, E. G., *Appl. Catal.* **43,** L5, (1988).
14. Barrage, M. C., Bonardt, J. L., and Fraissard, J., *Catal. Lett.* **5,** 143 (1990).
15. Miller, J. T., Meyers, B. L., and Ray, G. J., *J. Catal.* **128,** 436 (1991).
16. Tsiao, C., Dybowski, C., Gaffney, A. M., and Sofranko, J. A., *J. Catal.* **128,** 520 (1991).
17. Barrage, M. C., Bauer, F., Ernst, H., Fraissard, J., Freude, D., and Pfeifer, H., *Catal. Lett.* **6,** 201 (1990).
18. Derouane, E. G., Gilson, J. P., and Nagy, J. B., *Zeolites* **2,** 42 (1982).
19. van den Berg, J. P., Wolthuizen, J. P., Claque, A. D. H., Hays, G. R., Huis, R., and van Hooff, J. H. C., *J. Catal.* **80,** 130 (1983).
20. Neuber, M., Ernst, S., Geerts, H., Grobet, P. J., Jacobs, P. A., Kokotailo, G. T., and Weitkamp, J., *Stud. Surf. Sci. Catal.* **34,** 567 (1987).
21. Carlton, L., Copperthwaite, R. G., Hutchings, G. J., and Raynhardt, E. C., *J. Chem. Soc. Chem. Commun.*, 1008 (1986).
22. Lange, J. P., Gutsze, A., Allgeier, J., and Karge, H. G., *Appl. Catal.* **45,** 345 (1988).
23. Meinhold, R. H., and Bibby, D. M., *Zeolites* **10,** 121 (1990).
24. Chao, K. J., Tsai, T. C., Chen, M. S., and Wang, I., *J. Chem. Soc. Faraday Trans. 1* **77,** 547 (1981).
25. Liu, S. B., Wu, J. F., Ma, L. J., Lin, M. W., and Chen, T. L., *Collect. Czech. Chem. Commun.* **57,** 718 (1992); *J. Phys. Chem.* **96,** 8120 (1992).
26. Magnoux, P., Canaff, C., Machado, F., and Guisnet, M., *J. Catal.* **134,** 286 (1992).
27. Stothers, J. B., "Carbon-13 NMR Spectroscopy," p. 90. Academic Press, New York, 1972.
28. Copperthwaite, R. G., Hutchings, G., Johnston, P., and Orchard, S. W., *J. Chem. Soc. Chem. Commun.*, 644 (1985); *J. Chem. Soc. Faraday Trans. 1* **82,** 1007 (1986).
29. Nováková, J., Kubelková, L., Bosáček, V., and Mach, K., *Zeolites* **11,** 135 (1991).
30. Lammertsma, K., and Cerfontain, H., *J. Am. Chem. Soc.* **101,** 3618 (1979).
31. Lammertsma, K., *J. Am. Chem. Soc.* **103,** 2062 (1981).
32. Liu, S. B., Wu, J. F., Ma, L. J., Tsai, T. C., and Wang, I., *J. Catal.* **132,** 432 (1991).
33. Fraissard, J., Ito, T., Springuel-Huet, M. A., and Demarquay, J., *Stud. Surf. Sci. Catal.* **28,** 393 (1986).
34. Chen, Q., Springuel-Huet, M. A., Fraissard, J., Smith, M. L., Corbin, D. R., and Dybowski, C., *J. Phys. Chem.* **96,** 10914 (1992).
35. Bonardet, J. L., Barrage, M. C., Fraissard, J. P., Kubelková, L., Nováková, J., Ernst, H., and Freude, D., *Collect. Czech. Chem. Commun.* **57,** 733 (1992).
36. Förste, C., Germanus, A., Kärger, J., Pfeifer, H., Caro, J., Pilz, W., and Zikánová, A., *J. Chem. Soc. Faraday Trans. 1* **83,** 2301 (1987).
37. Portsmouth, R. L., and Gladden, L. F., *J. Chem. Soc. Chem. Commun.*, 512 (1992).
38. Hashimoto, K., Masuda, T., and Mori, T., *Chem. Eng. Sci.* **43,** 2275 (1988).